

# Numerical analysis of multicore photonic crystal fibers

Yanfeng Li (栗岩峰), Qingyue Wang (王清月), and Minglie Hu (胡明列)

Key Laboratory of Optoelectronic Information Technical Science, EMC; Ultrafast Laser Laboratory, College of Precision Instrument and Optoelectronics Engineering, Tianjin University, Tianjin 300072

Received April 28, 2003

A Galerkin's method-based numerical procedure is extended to obtain the modal field distribution of multicore photonic crystal fibers for the first time to our knowledge, which can reveal how the air hole size influences the mode coupling and how the coupling strength varies with wavelength. These results will be helpful in the future design of multicore photonic crystal fibers with proper guidance properties.

OCIS codes: 060.2270, 060.2310, 060.2400.

Photonic crystal fibers, also referred to as holey fibers or microstructured optical fibers, are the generic term for a new class of all-silica optical fibers whose cladding typically comprises a hexagonal array of air holes running along the entire length. Guiding cores are formed by one or more defects which are deliberately introduced into the lattice. Since the first photonic crystal fiber was fabricated in 1996<sup>[1]</sup>, photonic crystal fibers have attracted considerable research interest because they can offer a wide range of properties unattainable with conventional optical fibers. These properties include single-mode guidance over a wide spectral range<sup>[2]</sup>, anomalous dispersion at visible wavelengths<sup>[3]</sup>, mode size tailing<sup>[4]</sup> and others.

Photonic crystal fibers guide light by one of the two mechanisms, modified total internal reflection and photonic bandgap effect<sup>[5]</sup>. In the former case, light is guided along the silica core in a similar way as conventional optical fibers due to the difference between the higher refractive index of the core and the lower effective refractive index of the cladding. In the latter case, light propagation occurs as a result of the presence of the photonic bandgap in the periodic cladding.

Two or more cores in optical fibers are of particular interest for applications such as telecommunications, vector bend sensors and fiber couplers<sup>[5-12]</sup>. In such applications, photonic crystal fiber technology is preferable in that multicore structures can be produced by the stack-and-draw process with great geometrical precision and without additional fabrication effort.

However, the analysis of such novel fibers has been a challenge because of the complex refractive index profile in the cladding region. A number of methods, either vectorial or scalar, have been proposed to analyze photonic crystal fibers<sup>[6,13-16]</sup>, among which few have been used to study the multicore case<sup>[6,15]</sup>.

A Galerkin's method-based numerical procedure has been used to study single-core photonic crystal fibers<sup>[17]</sup>. In this letter, we extend this method to obtain the modal field distribution of multicore air-silica photonic crystal fibers. Taking a two-core photonic crystal fiber as an example, we study how the air hole size influences the mode coupling between the cores and how the coupling strength varies with wavelength. A three-core fiber is also studied as an illustration of the flexibility of the method.

The essence of this method is to reduce the problem of solving the scalar wave equation to a matrix eigenvalue problem. The calculation is performed over a rectangular area defined by  $x = [0, L_x]$  and  $y = [0, L_y]$ , as shown in Fig. 1. The electric field is expanded in terms of orthogonal basis functions in the form

$$\phi_{mn}(x, y) = \frac{2}{\sqrt{L_x L_y}} \sin\left(\frac{m\pi}{L_x} x\right) \sin\left(\frac{n\pi}{L_y} y\right). \quad (1)$$

The basis functions go to zero at the boundary and also satisfy the orthonormality condition over the area of calculation. By substituting the basis functions into the scalar wave equation

$$\frac{\partial^2 E}{\partial x^2} + \frac{\partial^2 E}{\partial y^2} + (n^2 - n_{\text{eff}}^2) k_0^2 E = 0, \quad (2)$$

and after some mathematical manipulation, a matrix eigenvalue problem can be derived

$$[F][A] = n_{\text{eff}}^2 [A], \quad (3)$$

where the matrix elements are

$$F_{klmn} = M_{klmn} + X_{klmn}, \quad (4)$$

$$M_{klmn} = \int_0^{L_x} \int_0^{L_y} \phi_{kl} n^2(x, y) \phi_{mn} dx dy, \quad (5)$$

$$X_{klmn} = -\frac{1}{k_0^2} \left[ \left(\frac{m\pi}{L_x}\right)^2 + \left(\frac{n\pi}{L_y}\right)^2 \right] \delta_{km} \delta_{ln}, \quad (6)$$

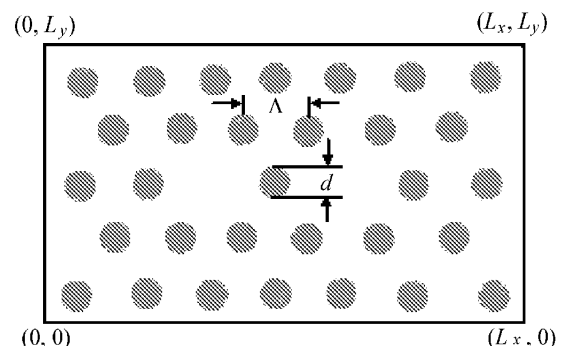


Fig. 1. Schematic of the area of calculation and a two-core photonic crystal fiber with parameters  $\Lambda$  and  $d$ .

$$A_{kl} = a_{kl}. \quad (7)$$

Note that we have corrected the mistakes in the expressions of the matrix elements given in Ref. [17].

The overlap integration in Eq. (5) can be simplified by utilizing the linearity nature of the integration, which has been explained in detail in Ref. [17]. The advantage of this procedure is that the overlap integration needs to be calculated only once for given fiber parameters  $\Lambda$  (hole-to-hole spacing or pitch) and  $d$  (hole diameter), as shown in Fig. 1. Additionally, the core positions can easily be taken into consideration in the algorithm in comparison with others methods, for example, the finite difference method<sup>[16]</sup>, which may need to be discretized once again.

Taking for example a two-core photonic crystal fiber where the cores are separated by one hole, we study by obtaining the modal field distribution how the air hole size influences mode coupling between the two cores and how the coupling strength varies with wavelength when the pitch  $\Lambda$  is fixed. Figure 2 shows the modal field distribution for two air hole sizes and two wavelengths, where each window is  $12\Lambda \times 7\Lambda$ . The two cores are in the  $x$  direction and separated by one hole which is at the center of each window.

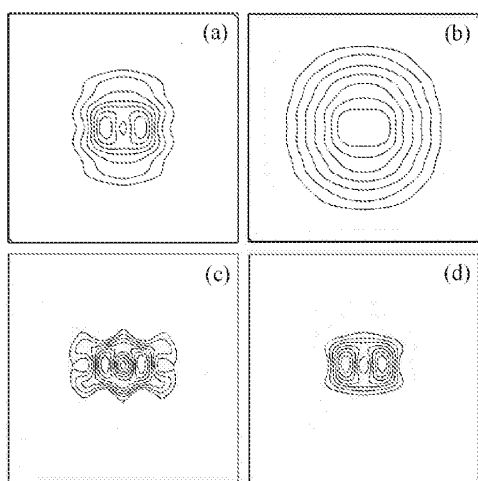


Fig. 2. Contour plots of the modal field distribution of the two-core photonic crystal fiber for  $\Lambda = 2 \mu\text{m}$ : (a)  $d = 0.2 \mu\text{m}$ ,  $\lambda = 800 \text{ nm}$ ; (b)  $d = 0.2 \mu\text{m}$ ,  $\lambda = 1.5 \mu\text{m}$ ; (c)  $d = 0.6 \mu\text{m}$ ,  $\lambda = 800 \text{ nm}$ ; (d)  $d = 0.6 \mu\text{m}$ ,  $\lambda = 1.5 \mu\text{m}$ .

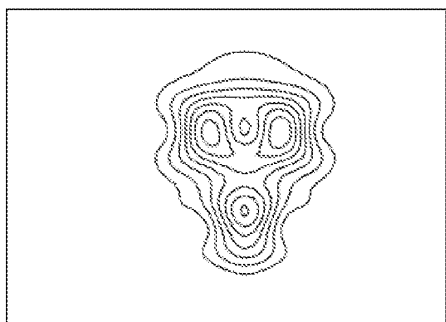


Fig. 3. Contour plot of the modal field distribution of the three-core photonic crystal fiber ( $\Lambda = 2 \mu\text{m}$ ,  $d = 0.6 \mu\text{m}$ , and  $\lambda = 1.5 \mu\text{m}$ ).

When the air holes are extremely small, the light confinement effect is not strong enough so that light penetrates further into the cladding region, as shown in Figs. 2(a) and (b). Because light at a longer wavelength can penetrate further into the air hole between the two cores, the two cores behave more like a single elliptical one, as shown in Fig. 2(b), while at a shorter wavelength, the role of the hole that separates the two cores is apparent, as shown in Fig. 2(a). As the air hole size is increased, the coupling strength decreases and the modal field is more confined around the two cores separately, as shown in Figs. 2(c) and 2(d). As it is easier for light at a shorter wavelength to escape into the cladding region through the silica bridges joining the air holes, the modal field for  $\lambda = 800 \text{ nm}$  in Fig. 2(c) is more complicated than that for  $\lambda = 1.5 \mu\text{m}$  in Fig. 2(d) in the cladding. It is clear that coupling is still stronger for  $\lambda = 1.5 \mu\text{m}$ , suggesting that weak coupling for a shorter wavelength may not be negligible for a longer wavelength in the present case.

The examined photonic crystal fiber has two cores separated by only one hole. We can easily extend this procedure to two-core photonic crystal fibers where the cores are separated by more than one hole and multicore photonic crystal fibers. To illustrate the flexibility of this method, Fig. 3 shows the modal field distribution of a three-core photonic crystal fiber where the three cores are separated by one hole and two of them are put above and the rest is put below. The size of the window is the same as in Fig. 2. The modal field is asymmetric as opposed to the symmetric arrangement case in Ref. [6] in which two holes separate the three cores. Thus, the flexibility of this numerical method makes it possible to design multicore photonic crystal fibers with proper guidance properties.

In conclusion, we have used a numerical tool to analyze multicore air-silica photonic crystal fibers. Efforts are made to investigate how mode coupling between the cores in multicore photonic crystal fibers is affected by the air hole size as well as the wavelength. Our results show that weak coupling between the cores at a shorter wavelength may not be negligible at a longer wavelength when one hole separates the cores. A three-core photonic crystal fiber is also studied. These results will help the design of multicore photonic crystal fibers where coupling may be desirable or should be avoided depending on the application.

This work was supported by the National Natural Science Foundation of China under Grant No. 60278003 and the National Key Basic Research Special Foundation of China under Grant No. G1999075201. Y. Li's e-mail address is li-yanfeng@163.com.

## References

1. J. C. Knight, T. A. Birks, P. St. J. Russell, and D. M. Atkin, *Opt. Lett.* **21**, 1547 (1996).
2. T. A. Birks, J. C. Knight, and P. St. J. Russell, *Opt. Lett.* **22**, 961 (1997).
3. J. C. Knight, J. Arriaga, T. A. Birks, A. Ortigosa-Blanch, W. J. Wadsworth, and P. St. J. Russell, *IEEE Photon. Technol. Lett.* **12**, 807 (2000).
4. J. C. Knight, T. A. Birks, R. F. Cregan, P. St. J. Russell, and J.-P. de Sandro, *Electron. Lett.* **34**, 1347 (1998).

5. B. J. Mangan, J. C. Knight, T. A. Birks, P. St. J. Russell, and A. H. Greenaway, *Electron. Lett.* **36**, 1358 (2000).
6. P. J. Roberts and T. J. Shepherd, *J. Opt. A: Pure Appl. Opt.* **3**, S133 (2001).
7. P. M. Blanchard, J. G. Burnett, G. R. G. Erry, A. H. Greenaway, P. Harrison, B. Mangan, J. C. Knight, P. St. J. Russell, M. J. Gander, R. McBride, and J. D. C. Jones, *Smart Mater. Struct.* **9**, 132 (2000).
8. E. Martin, B. J. Mangan, A. Diez, and P. St. J. Russell, in *Proceedings of ECOC 27*, 518 (2001).
9. B. J. Mangan, J. C. Knight, T. A. Birks, and P. St. J. Russell, in *Proceedings of QELS 1999* 271 (1999).
10. B. J. Mangan, J. C. Knight, T. A. Birks, and P. St. J. Russell, in *Proceedings of CLEO 1999* 559 (1999).
11. G. Kakarantzas, B. J. Mangan, T. A. Birks, J. C. Knight, and P. St. J. Russell, in *Proceedings of QELS 2001* 125 (2001).
12. W. N. MacPherson, J. D. C. Jones, B. J. Mangan, J. C. Knight, and P. St. J. Russell, in *Proceedings of Opt. Fiber Sensors Conf. 2002, Techn. Digest* 603 (2002).
13. T. M. Monro, D. J. Richardson, N. G. R. Broderick, and P. J. Bennett, *J. Lightwave Technol.* **17**, 1093 (1999).
14. A. Ferrando, E. Silvestre, J. J. Miret, P. Andrés, and M. V. Andrés, *Opt. Lett.* **24**, 276 (1999).
15. F. Fogli, L. Saccomandi, P. Bassi, G. Bellanca, and S. Trillo, *Opt. Express* **10**, 54 (2002).
16. Z. Zhu and T. G. Brown, *Opt. Express* **10**, 853 (2002).
17. J. Kim, Y. Chung, U. Paek, and D. Y. Kim, in *Proceedings of OECC 2000* 12B3 (2000).